Observation of Non-Markovian Spin Dynamics in a Jaynes-Cummings-Hubbard Model Using a Trapped-Ion Quantum Simulator

B.-W. Li[1,*] Q.-X. Mei[1,*] Y.-K. Wu[1,*] M.-L. Cai[1,2] Y. Wang[1] L. Yao[1,2] Z.-C. Zhou[1] and L.-M. Duan[1,†]

[1]*Center for Quantum Information, Institute for Interdisciplinary Information Sciences, Tsinghua University, Beijing 100084, People's Republic of China*
[2]*HYQ Co., Ltd., Beijing, 100176, People's Republic of China*

The Jaynes-Cummings-Hubbard (JCH) model is a fundamental many-body model for light-matter interaction. As a leading platform for quantum simulation, the trapped ion system has realized the JCH model for two to three ions. Here, we report the quantum simulation of the JCH model using up to 32 ions. We verify the simulation results even for large ion numbers by engineering low excitations and thus low effective dimensions; then we extend to 32 excitations for an effective dimension of 2^{77}, which is difficult for classical computers. By regarding the phonon modes as baths, we explore Markovian or non-Markovian spin dynamics in different parameter regimes of the JCH model, similar to quantum emitters in a structured photonic environment. We further examine the dependence of the non-Markovian dynamics on the effective Hilbert space dimension. Our Letter demonstrates the trapped ion system as a powerful quantum simulator for many-body physics and open quantum systems.

As the size and the controllability of the available quantum information processors advance [1,2], quantum simulation [3–5] has become a promising and convenient approach to understanding many-body quantum dynamics that are challenging for classical computers, for which various approximations have to be carefully designed and implemented due to the well-known "curse of dimensionality." Ion trap, one of the leading platforms for quantum information processing [1], has been widely applied in the quantum simulation of many-body spin models with long-range Ising or Heisenberg-type interactions [6–8] mediated by the spatial oscillation of the ions. Record-breaking experiments have simulated quantum dynamics of up to 53 spins [9], and properties such as phase transitions [9–12], frustration [13,14], information propagation [15–17], localization [18–21], and Floquet dynamics [22,23] have been examined. In these experiments, the quantized oscillation modes, also known as phonon modes, are only virtually excited through off-resonant laser driving. On the other hand, stronger driving close to phonon sidebands can explicitly excite the phonon states and interact them with the spins. Such schemes have found broad applications in quantum information processing [24–28], bosonic state engineering [29–31], and quantum transport [32–36]. Moreover, the inclusion of the phonon degrees of freedom opens up an avenue toward the richer phenomena in the spin-boson hybrid systems such as the quantum Rabi model [37–39] for a single ion and the Hubbard-like models [40–42] in the multi-ion cases.

Two prototypical many-body models with spin-boson interactions are the Jaynes-Cummings-Hubbard (JCH) model [40,41,43–49] and the Rabi-Hubbard (RH) model [42,50–53], both of which originate from cavity quantum electrodynamics systems but are well suited for the trapped ions owing to the strong and controllable spin-phonon coupling. The embracement of the spin and phonon states significantly increases the dimension of the effective Hilbert space, making these problems even more challenging for classical computers. Recently, equilibrium and dynamical properties of the RH model have been studied for up to 16 ions, which amounts to an effective dimension of 2^{57} [54]. In comparison, the JCH model possesses an additional U(1) symmetry and thus demonstrates essentially different properties: the ground state phase diagram of the JCH model now displays a multicritical point [47,48] similar to the Bose-Hubbard model [55–57], as opposed to the Ising universality class of the RH model [52,53]; the effective Hilbert space dimension is now governed by the conserved excitation number of the system, allowing a well-regulated study of the many-body dynamics versus the system dimension from a polynomial to an exponential scaling with the ion number. This also provides a natural test bed to directly verify the simulated Hamiltonian for large ion numbers, rather than the exponential cost for general systems [58–60] or to extrapolate from smaller systems. Furthermore, when regarding the phonon modes as an environment, the model resembles quantum emitters in a structured photonic background like a photonic crystal [61–64] where phenomena like thermalization [65], non-Markovian dynamics [66–70], collective radiation [68,71–73], and the dissipative generation of entanglement [74–77] can emerge. Previously, the JCH model has been
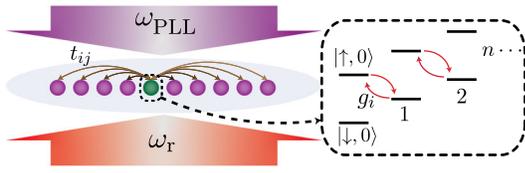
FIG. 1. Experimental scheme. Two counterpropagating global Raman laser beams are applied perpendicular to a chain of 2 to 32 ions to generate a Jaynes-Cummings-Hubbard (JCH) model Hamiltonian. The beat frequency of the Raman laser beams is tuned close to the red motional sideband, and is stabilized by a phase-locked loop (PLL). The internal state of each ion is coupled with its local oscillation by the Raman laser beams as a Jaynes-Cummings model, and these local oscillation modes of individual ions are further coupled by their Coulomb interaction.

implemented in ion trap in small scales using two [78,79] or three ions [80] for observing the hopping and blockade of phonons and the signature of quantum phase transition. However, many of the aforementioned dynamical properties require large system sizes and remain to be demonstrated in the experiment.

In this Letter, we report the quantum simulation of a JCH model with long-range interaction using a trapped chain of up to 32 ions. The successful simulation of the JCH Hamiltonian is verified directly for large ion numbers by engineering the low total excitation number of the system. Then we demonstrate the change from the Markovian to non-Markovian dynamics by tuning the frequency of the spins into different locations of the phonon spectrum. We further adjust the effective dimension of the system via the ion number and the excitation number, and observe that the non-Markovian dynamics persists for large systems. With up to 32 excitations in 32 ions, an effective Hilbert space dimension above 2^{77} is achieved, which is challenging for existing supercomputers. Our Letter showcases the trapped ion system as a powerful quantum simulator of spin-boson coupled systems and open quantum systems with a bosonic environment.

Our experimental setup is shown schematically in Fig. 1 using a chain of $^{171}\mathrm{Yb}^+$ ions in a linear Paul trap. The internal electronic levels $|\downarrow\rangle \equiv |S_{1/2}, F = 0, m_F = 0\rangle$ and $|\uparrow\rangle \equiv |S_{1/2}, F = 1, m_F = 0\rangle$ of each ion encode an individual spin. The local phonon modes of the ion chain naturally possess long-range hopping terms due to the Coulomb interaction. We further turn on the on-site Jaynes-Cummings interaction via a pair of counterpropagating 355 nm global Raman beams whose beat frequency is tuned close to the red motional sideband. Moving into an interaction picture, the Hamiltonian of the system is governed by a JCH model

$$H = \sum_i \left[\frac{\Delta}{2} \sigma_z^i + \omega_i a_i^\dagger a_i + g_i (\sigma_+^i a_i + a_i^\dagger \sigma_-^i) \right]$$
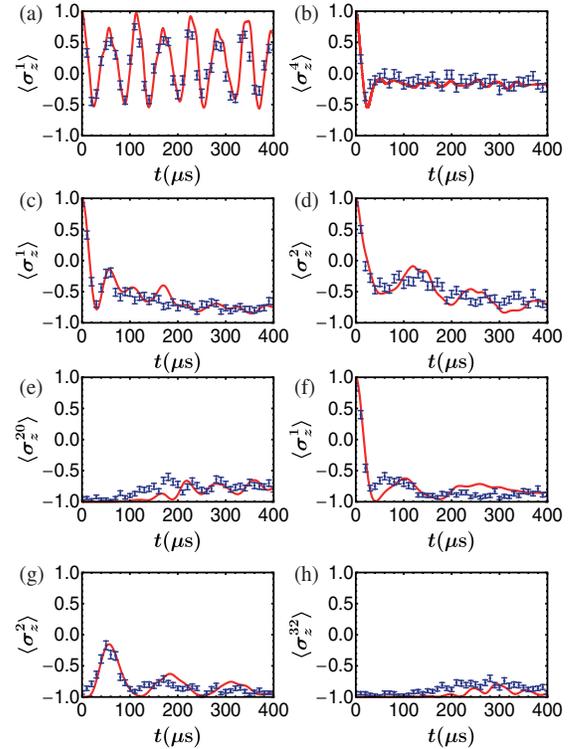$$+ \sum_{i<j} t_{ij} (a_i^\dagger a_j + a_j^\dagger a_i), \qquad (1)$$

FIG. 2. Comparison between experimental spin dynamics and theoretical prediction for small Hilbert space dimensions. Blue dots (with error bars representing one standard deviation) are experimentally measured $\langle\sigma_z^i(t)\rangle$ for individual ions, and the red curves are the corresponding theoretical results by exact diagonalization with no fitting parameters. (a) Two ions initialized in $|\uparrow, 0\rangle^{\otimes 2}$ (two total excitations) under $\Delta = -2\pi \times 60$ kHz and $g = 2\pi \times 11.6$ kHz. The evolutions of the two ions are symmetric so only one is plotted. (b) Similar plot for a central ion (ion 4, labeled by 1 to N from left to right) in an $N = 8$ chain under $\Delta = -2\pi \times 60$ kHz and $g = 2\pi \times 11.5$ kHz with the initial state $|\uparrow, 0\rangle^{\otimes 8}$ (8 excitations). (c)–(e) $N = 20$ ions with two total excitations initialized in $|\uparrow, 0\rangle^{\otimes 2} \otimes |\downarrow, 0\rangle^{\otimes 18}$ under $\Delta = -2\pi \times 5$ kHz and $g = 2\pi \times 10$ kHz. (c) Ion 1 and (d) ion 2 are the two ions being excited on the left of the chain, while (e) ion 20 is the ion on the right. (f)–(h) $N = 32$ ions with one total excitation initialized in $|\uparrow, 0\rangle \otimes |\downarrow, 0\rangle^{\otimes 31}$ under $\Delta = -2\pi \times 5$ kHz and $g = 2\pi \times 11.6$ kHz. (f) is for the excited ion 1 on the left, (g) for its neighbor ion 2, and (h) for the ion 32 on the other end of the chain.

where Δ is the spin frequency set by the Raman laser detuning from the motional sideband, ω_i the local phonon frequency in the interaction picture, g_i the spin-phonon coupling on the ith ion, and t_{ij} the phonon hopping rates. Since g_i is not uniform due to the finite laser beam width, we describe it by a maximal coupling g for the central ion and the others can be deduced from the Gaussian beam profile of the laser. More details about the derivation of the Hamiltonian and the calibration of the model parameters can be found in Supplemental Material [81]. Note that Δ and ω_i can be shifted by a same constant without affecting
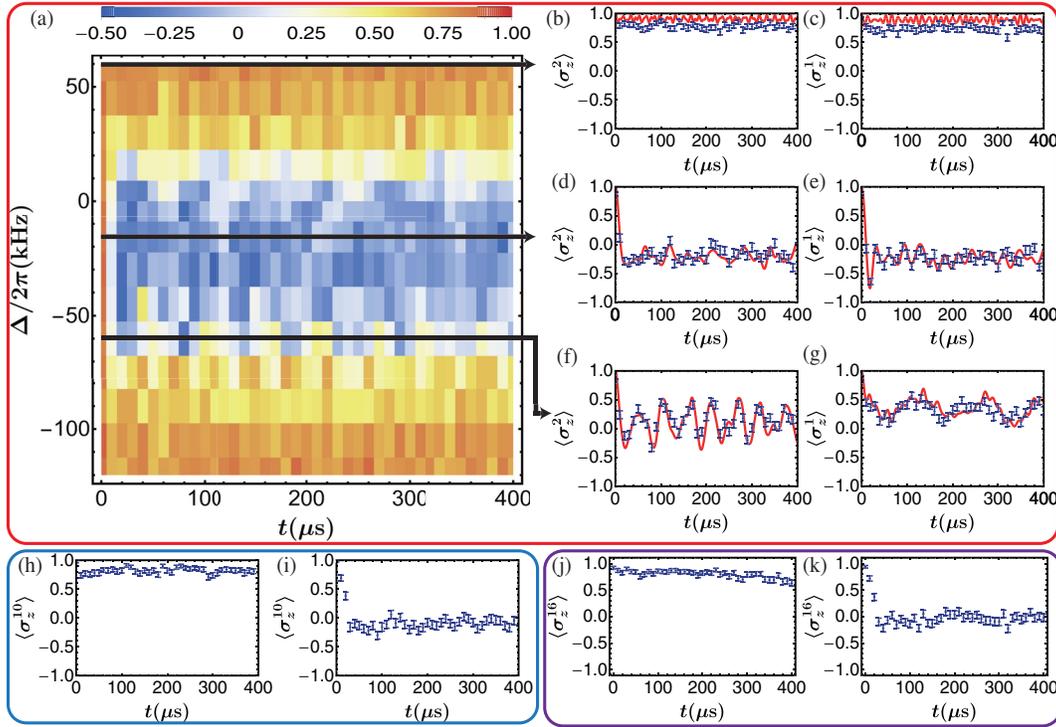
FIG. 3.   Markovian and non-Markovian spin dynamics in different regimes of the JCH model. We initialize the system at $|\uparrow, 0\rangle^{\otimes N}$ with $M = N$ total excitations. We fix $g = 2\pi \times 12.9$ kHz and tune Δ to observe different spin dynamics $\langle \sigma_z^i(t) \rangle$. (a) Experimental results for $N = 4$ ions with Δ ranging from $-2\pi \times 120$ kHz to $2\pi \times 60$ kHz. The response strongly depends on the location of Δ with respect to the phonon band from $-2\pi \times 52$ kHz to zero. (b)–(g) Dynamics in different parameter regimes in (a) as indicated by black horizontal arrows for the central (left panel) and edge (right panel) ions. Red curves are the theoretical results from exact diagonalization. (h),(i) Measured spin dynamics for a central ion of an $N = 20$ chain with $\Delta = 2\pi \times 30$ kHz (outside band) and $-2\pi \times 5$ kHz (near band edge), respectively. (j),(k) Similar plots for an $N = 32$ chain with $\Delta = 2\pi \times 30$ kHz and $-2\pi \times 5$ kHz, respectively.

any relevant dynamics owing to the U(1) symmetry of the Hamiltonian. This symmetry also results in the conservation of total spin and phonon excitations in the system, which is in stark contrast to the RH model [54].

First, we verify the successful quantum simulation of the JCH model by measuring the spin dynamics and comparing with the theoretical predictions in small system sizes. For N ions and M total excitations, the effective dimension of the Hilbert space is given by

$$D = \sum_{k=0}^{\min(N,M)} C(N, k) \times C(N + M - k - 1, N - 1), \quad (2)$$

where $C(n, m) \equiv n!/[m!(n - m)!]$ is the combination number to choose m items from n elements. Although D generally increases rapidly with N and M (for $N = M = 32$ we have $D > 2^{77}$), it turns out that even under large ion number $N = 32$, the classical simulation is still feasible for small values of M. This allows us to directly verify the correctness of the quantum simulation results at large system sizes rather than to extrapolate from smaller systems. In Fig. 2 we plot the measured spin dynamics

for $N = 2$ and $N = 8$ ions with $M = N$ total excitations, and for $N = 20$ and $N = 32$ ions with $M = 2$ and $M = 1$ total excitations, respectively. To create $M = N$ total excitations, we initialize the system in $|\psi_0\rangle = |\downarrow, 0\rangle^{\otimes N}$ by sideband cooling and optical pumping [81,83], and then we apply a global microwave π pulse to get $|\uparrow, 0\rangle^{\otimes N}$. As for the $M = 1$ or $M = 2$ cases, after initializing $|\psi_0\rangle$, we use a combination of global microwave pulses and a focused 355 nm Raman beam to flip the target ions (which we choose as ions on the edges because they have larger interion spacings and thus less crosstalk errors) into $|\uparrow\rangle$ [81]. After preparing an initial state with the desired total excitation number, we turn on the JCH Hamiltonian and measure $\langle \sigma_z^i(t) \rangle$ for individual spins. As we can see, for various system sizes, excitation numbers as well as ion locations, the measured spin dynamics agrees well with the theoretical results with no free parameters (all parameters are calibrated in advance as described in Supplemental Material [81]). There is a small systematic discrepancy for $N = 20$ and $N = 32$ where we prepare one or two spin excitations on the one end of the chain while the curve for the ion on the opposite end rises earlier than the theoretical prediction. This is mainly caused by the imperfect sideband

cooling such that with small probability there are additional phonon excitations in the system that can quickly convert into the spin excitation of the distant ions [81].

After demonstrating the successful quantum simulation of the JCH model, now we regard the phonon modes as a structured bosonic environment and examine the non-Markovian dynamics of the spins. This problem is similar to quantum emitters in a photonic crystal [61–64], and it has been predicted [64,68] and demonstrated [70] that by placing the spins at different locations of the bosonic spectrum, strikingly different behavior can occur. In Fig. 3 we measure the spin dynamics for $N = 4, 20, 32$ and $M = N$ from the initial state $|\uparrow, 0\rangle^{\otimes N}$. For $N = 4$ ions the frequencies of the collective phonon modes (note that they are different from the local phonon frequencies ω_i) are distributed from $-2\pi \times 52$ kHz to 0 in the interaction picture [81]. As we can see in Fig. 3(a), when tuning Δ within this phonon band, we observe significant decay in the individual $\langle \sigma_z^i(t) \rangle$ away from their initial values of one, while outside the phonon band the response is much weaker. We further plot the dynamics for typical Δ in Figs. 3(b)–3(g) together with the theoretical predictions under the same parameters. Far outside the phonon band [(b),(c) $\Delta = 2\pi \times 60$ kHz], there is almost no decay in $\langle \sigma_z^i(t) \rangle$ due to the large detuning between the spins and phonons; inside the band [(d),(e) $\Delta = -2\pi \times 15$ kHz] a fast decay is observed (predicted to be exponential in the continuum limit [64,68]) with small oscillations; and near the edge of the band [(f),(g) $\Delta = -2\pi \times 60$ kHz] there is non-Markovian dynamics of both decay and oscillation, resulting from a mixture of the dynamics inside and outside the phonon band. We observe similar behavior for larger ion numbers $N = 20$ (h),(i) and $N = 32$ (j),(k) as well: outside the phonon band [(h),(j) $\Delta = 2\pi \times 30$ kHz] the spin population evolves slowly; while near the band edge we get non-Markovian dynamics of fast decay together with long-term oscillation, namely collapse and revival in the spin population.

Intuitively, one would expect a monotonic decrease in the revival signal as the dimension of the effective Hilbert space increases. However, the non-Markovian dynamics is known to persist even for a continuum of the environment [68,70]. To resolve this inconsistency, in Fig. 4 we systematically examine this dependence on the system dimension. We plot the spin dynamics for $N = 4$ (a),(b), $N = 20$ (c),(d), and $N = 32$ (e),(f) ions with $M = 1$ (left) and $M = 2$ (right) total excitations. The change is most significant when increasing from $N = 4, M = 1$ to $N = 4, M = 2$ or to $N = 20, M = 1$, while for larger system sizes the curves are similar and there can even be additional revival signals owing to the added excitation number at $M = 2$, which are also confirmed by the theoretical calculation as the red curves in these plots. This can be explained by the localization of the excitations near the individual spins when tuned close to the band edge [68]
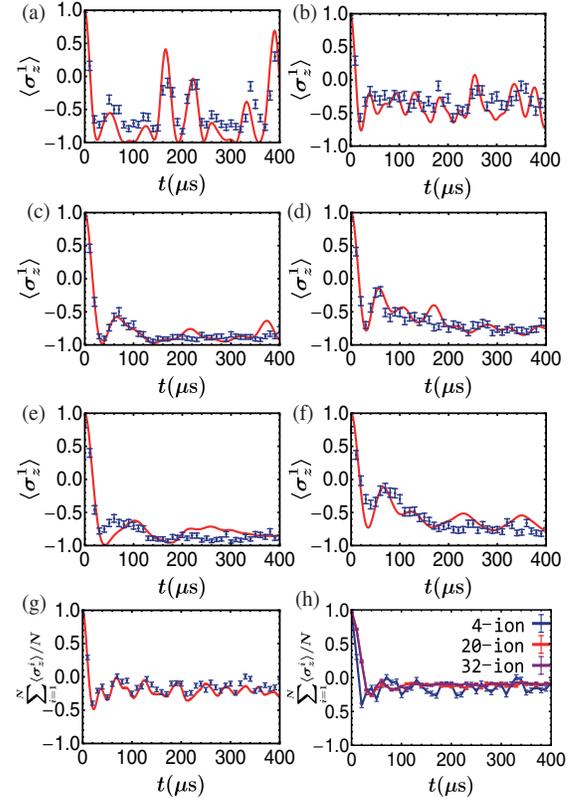

FIG. 4. Collapse and revival in spin dynamics under various Hilbert space dimensions. (a) and (b) Experimental data (blue dots with error bars for one standard deviation) and theoretical results (red curves) for an initially excited ion in an $N = 4$ chain with (a) one and (b) two total excitations, respectively. Here, we choose $\Delta = -2\pi \times 10$ kHz and $g = 2\pi \times 11.5$ kHz. (c)–(f) Similar plots for (c) and (d) $N = 20$ ions under $\Delta = -2\pi \times 5$ kHz and $g = 2\pi \times 10$ kHz, and (e),(f) $N = 32$ ions under $\Delta = -2\pi \times 5$ kHz and $g = 2\pi \times 11.6$ kHz. The system has (c),(e) one or (d),(f) two total excitations. (g) The average spin dynamics $\sum_i \langle \sigma_z^i(t) \rangle / N$ under the parameters of (a),(b) with all the spins initialized in $|\uparrow\rangle$. (h) The average spin dynamics for $N = 4, 20, 32$ ions with $M = N$ total excitations. The $N = 4$ case is the same as (g). For $N = 20$ and $N = 32$ ions with N excitations, numerical calculation using exact diagonalization is intractable. Hence, in this case the theoretical curves are not plotted, and the data points are directly connected to guide the eyes.

such that the relevant phonon environment ceases to further scale up with the system sizes and thus the dynamics becomes similar for large N. Similar phenomena are also observed for average spin dynamics $\sum_i \langle \sigma_z^i(t) \rangle / N$ when we prepare $M = N$ total excitations. In Fig. 4(g) we observe a reduction in the oscillation amplitude for $N = 4$ ions compared with (a) and (b), and there is a further reduction to $N = 20$ as shown in Fig. 4(h). However, the curves for $N = 20$ and $N = 32$ are again similar and show non-Markovian revivals (see Supplemental Material for a larger plot [81]). Note that in (h) the data points are directly connected to guide the eye, because exact diagonalization for the large Hilbert space dimensions is not feasible.

In summary, we have demonstrated quantum simulation of the JCH model using up to 32 ions and up to 32 total excitations, which amounts to 2^{77} dimensional Hilbert space. The conservation of excitation number in this model allows us to adjust its effective dimension, thus providing efficient verification of the quantum simulation results even for large system sizes. Similar schemes shall also work for the quantum simulation of other models where under certain parameters the effective dimension is governed by a conservation law. With this tool, we observe the change from Markovian to non-Markovian spin dynamics by tuning the spin frequencies to different locations of the phonon band. We further study the dependence of the collapse and revival signals versus the effective dimension of the Hilbert space, and find similar dynamics for large system sizes which can result from localization in the system. Our Letter demonstrates the trapped ion quantum simulator a powerful platform for rich properties in spin-boson coupled systems and open quantum systems with structured bosonic environments.

---

[*]These authors contributed equally to this work.
[†]lmduan@tsinghua.edu.cn

[1] C. D. Bruzewicz, J. Chiaverini, R. McConnell, and J. M. Sage, Trapped-ion quantum computing: Progress and challenges, Appl. Phys. Rev. **6**, 021314 (2019).

[2] H.-L. Huang, D. Wu, D. Fan, and X. Zhu, Superconducting quantum computing: A review, Sci. China Inf. Sci. **63**, 180501 (2020).

[3] R. P. Feynman, Simulating physics with computers, in *Feynman and Computation* (CRC Press, Boca Raton, 2018), pp. 133–153.

[4] I. M. Georgescu, S. Ashhab, and F. Nori, Quantum simulation, Rev. Mod. Phys. **86**, 153 (2014).

[5] J. I. Cirac and P. Zoller, Goals and opportunities in quantum simulation, Nat. Phys. **8**, 264 (2012).

[6] D. Porras and J. I. Cirac, Effective Quantum Spin Systems with Trapped Ions, Phys. Rev. Lett. **92**, 207901 (2004).

[7] R. Blatt and C. F. Roos, Quantum simulations with trapped ions, Nat. Phys. **8**, 277 (2012).

[8] C. Monroe, W. C. Campbell, L.-M. Duan, Z.-X. Gong, A. V. Gorshkov, P. W. Hess, R. Islam, K. Kim, N. M. Linke, G. Pagano, P. Richerme, C. Senko, and N. Y. Yao, Programmable quantum simulations of spin systems with trapped ions, Rev. Mod. Phys. **93**, 025001 (2021).

[9] J. Zhang, G. Pagano, P. W. Hess, A. Kyprianidis, P. Becker, H. Kaplan, A. V. Gorshkov, Z.-X. Gong, and C. Monroe, Observation of a many-body dynamical phase transition with a 53-qubit quantum simulator, Nature (London) **551**, 601 (2017).

[10] A. Friedenauer, H. Schmitz, J. T. Glueckert, D. Porras, and T. Schätz, Simulating a quantum magnet with trapped ions, Nat. Phys. **4**, 757 (2008).

[11] R. Islam, E. Edwards, K. Kim, S. Korenblit, C. Noh, H. Carmichael, G.-D. Lin, L.-M. Duan, C.-C. J. Wang, J. Freericks et al., Onset of a quantum phase transition with a trapped ion quantum simulator, Nat. Commun. **2**, 377 (2011).

[12] P. Jurcevic, H. Shen, P. Hauke, C. Maier, T. Brydges, C. Hempel, B. P. Lanyon, M. Heyl, R. Blatt, and C. F. Roos, Direct Observation of Dynamical Quantum Phase Transitions in an Interacting Many-Body System, Phys. Rev. Lett. **119**, 080501 (2017).

[13] K. Kim, M.-S. Chang, S. Korenblit, R. Islam, E. E. Edwards, J. K. Freericks, G.-D. Lin, L.-M. Duan, and C. Monroe, Quantum simulation of frustrated Ising spins with trapped ions, Nature (London) **465**, 590 (2010).

[14] R. Islam, C. Senko, W. C. Campbell, S. Korenblit, J. Smith, A. Lee, E. E. Edwards, C.-C. J. Wang, J. K. Freericks, and C. Monroe, Emergence and frustration of magnetism with variable-range interactions in a quantum simulator, Science **340**, 583 (2013).

[15] P. Richerme, Z.-X. Gong, A. Lee, C. Senko, J. Smith, M. Foss-Feig, S. Michalakis, A. V. Gorshkov, and C. Monroe, Non-local propagation of correlations in quantum systems with long-range interactions, Nature (London) **511**, 198 (2014).

[16] P. Jurcevic, B. P. Lanyon, P. Hauke, C. Hempel, P. Zoller, R. Blatt, and C. F. Roos, Quasiparticle engineering and entanglement propagation in a quantum many-body system, Nature (London) **511**, 202 (2014).

[17] M. K. Joshi, A. Elben, B. Vermersch, T. Brydges, C. Maier, P. Zoller, R. Blatt, and C. F. Roos, Quantum Information Scrambling in a Trapped-Ion Quantum Simulator with Tunable Range Interactions, Phys. Rev. Lett. **124**, 240505 (2020).

[18] J. Smith, A. Lee, P. Richerme, B. Neyenhuis, P. W. Hess, P. Hauke, M. Heyl, D. A. Huse, and C. Monroe, Many-body localization in a quantum simulator with programmable random disorder, Nat. Phys. **12**, 907 (2016).

[19] T. Brydges, A. Elben, P. Jurcevic, B. Vermersch, C. Maier, B. P. Lanyon, P. Zoller, R. Blatt, and C. F. Roos, Probing Renyi entanglement entropy via randomized measurements, Science **364**, 260 (2019).

[20] C. Maier, T. Brydges, P. Jurcevic, N. Trautmann, C. Hempel, B. P. Lanyon, P. Hauke, R. Blatt, and C. F. Roos, Environment-Assisted Quantum Transport in a 10-Qubit Network, Phys. Rev. Lett. **122**, 050501 (2019).

[21] W. Morong, F. Liu, P. Becker, K. Collins, L. Feng, A. Kyprianidis, G. Pagano, T. You, A. Gorshkov, and C. Monroe, Observation of Stark many-body localization without disorder, Nature (London) **599**, 393 (2021).

[22] J. Zhang, P. Hess, A. Kyprianidis, P. Becker, A. Lee, J. Smith, G. Pagano, I.-D. Potirniche, A. C. Potter, A. Vishwanath et al., Observation of a discrete time crystal, Nature (London) **543**, 217 (2017).

[23] A. Kyprianidis, F. Machado, W. Morong, P. Becker, K. S. Collins, D. V. Else, L. Feng, P. W. Hess, C. Nayak, G. Pagano, N. Y. Yao, and C. Monroe, Observation of a prethermal discrete time crystal, Science **372**, 1192 (2021).

[24] J. I. Cirac and P. Zoller, Quantum Computations with Cold Trapped Ions, Phys. Rev. Lett. **74,** 4091 (1995).

[25] A. Sørensen and K. Mølmer, Entanglement and quantum computation with ions in thermal motion, Phys. Rev. A **62,** 022311 (2000).

[26] G. Milburn, S. Schneider, and D. James, Ion trap quantum computing with warm ions, Fortschr. Phys. **48,** 801 (2000).

[27] S.-L. Zhu, C. Monroe, and L.-M. Duan, Trapped Ion Quantum Computation with Transverse Phonon Modes, Phys. Rev. Lett. **97,** 050505 (2006).

[28] D. Leibfried, B. DeMarco, V. Meyer, D. Lucas, M. Barrett, J. Britton, W. M. Itano, B. Jelenković, C. Langer, T. Rosenband *et al.*, Experimental demonstration of a robust, high-fidelity geometric two ion-qubit phase gate, Nature (London) **422,** 412 (2003).

[29] A. Ben-Kish, B. DeMarco, V. Meyer, M. Rowe, J. Britton, W. M. Itano, B. M. Jelenković, C. Langer, D. Leibfried, T. Rosenband, and D. J. Wineland, Experimental Demonstration of a Technique to Generate Arbitrary Quantum Superposition States of a Harmonically Bound Spin-1/2 Particle, Phys. Rev. Lett. **90,** 037902 (2003).

[30] M. Um, J. Zhang, D. Lv, Y. Lu, S. An, J.-N. Zhang, H. Nha, M. Kim, and K. Kim, Phonon arithmetic in a trapped ion system, Nat. Commun. **7,** 11410 (2016).

[31] D. Kienzler, H.-Y. Lo, V. Negnevitsky, C. Flühmann, M. Marinelli, and J. P. Home, Quantum Harmonic Oscillator State Control in a Squeezed Fock Basis, Phys. Rev. Lett. **119,** 033602 (2017).

[32] A. Bermudez, M. Bruderer, and M. B. Plenio, Controlling and Measuring Quantum Transport of Heat in Trapped-Ion Crystals, Phys. Rev. Lett. **111,** 040601 (2013).

[33] M. Ramm, T. Pruttivarasin, and H. Häffner, Energy transport in trapped ion chains, New J. Phys. **16,** 063062 (2014).

[34] A. Abdelrahman, O. Khosravani, M. Gessner, A. Buchleitner, H.-P. Breuer, D. Gorman, R. Masuda, T. Pruttivarasin, M. Ramm, P. Schindler *et al.*, Local probe of single phonon dynamics in warm ion crystals, Nat. Commun. **8,** 15712 (2017).

[35] D. J. Gorman, B. Hemmerling, E. Megidish, S. A. Moeller, P. Schindler, M. Sarovar, and H. Haeffner, Engineering Vibrationally Assisted Energy Transfer in a Trapped-Ion Quantum Simulator, Phys. Rev. X **8,** 011038 (2018).

[36] M. Tamura, T. Mukaiyama, and K. Toyoda, Quantum Walks of a Phonon in Trapped Ions, Phys. Rev. Lett. **124,** 200501 (2020).

[37] P. Forn-Díaz, L. Lamata, E. Rico, J. Kono, and E. Solano, Ultrastrong coupling regimes of light-matter interaction, Rev. Mod. Phys. **91,** 025005 (2019).

[38] D. Lv, S. An, Z. Liu, J.-N. Zhang, J. S. Pedernales, L. Lamata, E. Solano, and K. Kim, Quantum Simulation of the Quantum Rabi Model in a Trapped Ion, Phys. Rev. X **8,** 021027 (2018).

[39] M.-L. Cai, Z.-D. Liu, W.-D. Zhao, Y.-K. Wu, Q.-X. Mei, Y. Jiang, L. He, X. Zhang, Z.-C. Zhou, and L.-M. Duan, Observation of a quantum phase transition in the quantum Rabi model with a single trapped ion, Nat. Commun. **12,** 1126 (2021).

[40] A. D. Greentree, C. Tahan, J. H. Cole, and L. C. Hollenberg, Quantum phase transitions of light, Nat. Phys. **2,** 856 (2006).

[41] D. G. Angelakis, M. F. Santos, and S. Bose, Photon-blockade-induced Mott transitions and *XY* spin models in coupled cavity arrays, Phys. Rev. A **76,** 031805(R) (2007).

[42] M. Schiró, M. Bordyuh, B. Öztop, and H. E. Türeci, Phase Transition of Light in Cavity QED Lattices, Phys. Rev. Lett. **109,** 053601 (2012).

[43] M. J. Hartmann, F. G. S. L. Brandão, and M. B. Plenio, Strongly interacting polaritons in coupled arrays of cavities, Nat. Phys. **2,** 849 (2006).

[44] D. Rossini and R. Fazio, Mott-Insulating and Glassy Phases of Polaritons in 1D Arrays of Coupled Cavities, Phys. Rev. Lett. **99,** 186401 (2007).

[45] E. K. Irish, C. D. Ogden, and M. S. Kim, Polaritonic characteristics of insulator and superfluid states in a coupled-cavity array, Phys. Rev. A **77,** 033801 (2008).

[46] M. I. Makin, J. H. Cole, C. Tahan, L. C. L. Hollenberg, and A. D. Greentree, Quantum phase transitions in photonic cavities with two-level systems, Phys. Rev. A **77,** 053819 (2008).

[47] J. Koch and K. Le Hur, Superfluid-Mott-insulator transition of light in the Jaynes-Cummings lattice, Phys. Rev. A **80,** 023811 (2009).

[48] S. Schmidt and G. Blatter, Strong Coupling Theory for the Jaynes-Cummings-Hubbard Model, Phys. Rev. Lett. **103,** 086403 (2009).

[49] P. A. Ivanov, S. S. Ivanov, N. V. Vitanov, A. Mering, M. Fleischhauer, and K. Singer, Simulation of a quantum phase transition of polaritons with trapped ions, Phys. Rev. A **80,** 060301(R) (2009).

[50] M.-J. Hwang and M.-S. Choi, Large-scale maximal entanglement and Majorana bound states in coupled circuit quantum electrodynamic systems, Phys. Rev. B **87,** 125404 (2013).

[51] G. Zhu, S. Schmidt, and J. Koch, Dispersive regime of the Jaynes-Cummings, and Rabi lattice, New J. Phys. **15,** 115002 (2013).

[52] M. Schiró, M. Bordyuh, B. Öztop, and H. E. Türeci, Quantum phase transition of light in the Rabi-Hubbard model, J. Phys. B **46,** 224021 (2013).

[53] T. Flottat, F. Hébert, V. G. Rousseau, and G. G. Batrouni, Quantum Monte Carlo study of the Rabi-Hubbard model, Eur. Phys. J. D **70,** 213 (2016).

[54] Q.-X. Mei, B.-W. Li, Y.-K. Wu, M.-L. Cai, Y. Wang, L. Yao, Z.-C. Zhou, and L.-M. Duan, Experimental Realization of the Rabi-Hubbard Model with Trapped Ions, Phys. Rev. Lett. **128,** 160504 (2022).

[55] M. P. A. Fisher, P. B. Weichman, G. Grinstein, and D. S. Fisher, Boson localization and the superfluid-insulator transition, Phys. Rev. B **40,** 546 (1989).

[56] D. Jaksch, C. Bruder, J. I. Cirac, C. W. Gardiner, and P. Zoller, Cold Bosonic Atoms in Optical Lattices, Phys. Rev. Lett. **81,** 3108 (1998).

[57] I. Bloch, J. Dalibard, and W. Zwerger, Many-body physics with ultracold gases, Rev. Mod. Phys. **80,** 885 (2008).

[58] A. Elben, B. Vermersch, R. van Bijnen, C. Kokail, T. Brydges, C. Maier, M. K. Joshi, R. Blatt, C. F. Roos, and P. Zoller, Cross-Platform Verification of Intermediate Scale Quantum Devices, Phys. Rev. Lett. **124,** 010504 (2020).

[59] J. Carrasco, A. Elben, C. Kokail, B. Kraus, and P. Zoller, Theoretical and experimental perspectives of quantum verification, PRX Quantum **2**, 010102 (2021).

[60] D. Zhu, Z.-P. Cian, C. Noel, A. Risinger, D. Biswas, L. Egan, Y. Zhu, A. M. Green, C. H. Alderete, N. H. Nguyen, Q. Wang, A. Maksymov, Y. Nam, M. Cetina, N. M. Linke, M. Hafezi, and C. Monroe, Cross-platform comparison of arbitrary quantum computations, arXiv:2107.11387.

[61] S. John and T. Quang, Spontaneous emission near the edge of a photonic band gap, Phys. Rev. A **50**, 1764 (1994).

[62] J. D. Thompson, T. G. Tiecke, N. P. de Leon, J. Feist, A. V. Akimov, M. Gullans, A. S. Zibrov, V. Vuletić, and M. D. Lukin, Coupling a single trapped atom to a nanoscale optical cavity, Science **340**, 1202 (2013).

[63] A. Goban, C.-L. Hung, S.-P. Yu, J. Hood, J. Muniz, J. Lee, M. Martin, A. McClung, K. Choi, D. E. Chang *et al.*, Atom–light interactions in photonic crystals, Nat. Commun. **5**, 3808 (2014).

[64] A. González-Tudela and J. I. Cirac, Quantum Emitters in Two-Dimensional Structured Reservoirs in the Nonperturbative Regime, Phys. Rev. Lett. **119**, 143602 (2017).

[65] G. Clos, D. Porras, U. Warring, and T. Schaetz, Time-Resolved Observation of Thermalization in an Isolated Quantum System, Phys. Rev. Lett. **117**, 170401 (2016).

[66] K. H. Madsen, S. Ates, T. Lund-Hansen, A. Löffler, S. Reitzenstein, A. Forchel, and P. Lodahl, Observation of Non-Markovian Dynamics of a Single Quantum Dot in a Micropillar Cavity, Phys. Rev. Lett. **106**, 233601 (2011).

[67] U. Hoeppe, C. Wolff, J. Küchenmeister, J. Niegemann, M. Drescher, H. Benner, and K. Busch, Direct Observation of Non-Markovian Radiation Dynamics in 3D Bulk Photonic Crystals, Phys. Rev. Lett. **108**, 043603 (2012).

[68] A. González-Tudela and J. I. Cirac, Markovian and non-Markovian dynamics of quantum emitters coupled to two-dimensional structured reservoirs, Phys. Rev. A **96**, 043811 (2017).

[69] H. Z. Shen, S. Xu, H. T. Cui, and X. X. Yi, Non-Markovian dynamics of a system of two-level atoms coupled to a structured environment, Phys. Rev. A **99**, 032101 (2019).

[70] V. S. Ferreira, J. Banker, A. Sipahigil, M. H. Matheny, A. J. Keller, E. Kim, M. Mirhosseini, and O. Painter, Collapse and Revival of an Artificial Atom Coupled to a Structured Photonic Reservoir, Phys. Rev. X **11**, 041043 (2021).

[71] A. F. van Loo, A. Fedorov, K. Lalumière, B. C. Sanders, A. Blais, and A. Wallraff, Photon-mediated interactions between distant artificial atoms, Science **342**, 1494 (2013).

[72] A. Goban, C.-L. Hung, J. D. Hood, S.-P. Yu, J. A. Muniz, O. Painter, and H. J. Kimble, Superradiance for Atoms Trapped along a Photonic Crystal Waveguide, Phys. Rev. Lett. **115**, 063601 (2015).

[73] N. V. Corzo, B. Gouraud, A. Chandra, A. Goban, A. S. Sheremet, D. V. Kupriyanov, and J. Laurat, Large Bragg Reflection from One-Dimensional Chains of Trapped Atoms Near a Nanoscale Waveguide, Phys. Rev. Lett. **117**, 133603 (2016).

[74] C. Gonzalez-Ballestero, F. J. García-Vidal, and E. Moreno, Non-Markovian effects in waveguide-mediated entanglement, New J. Phys. **15**, 073015 (2013).

[75] B. Bellomo, R. Lo Franco, and G. Compagno, Non-Markovian Effects on the Dynamics of Entanglement, Phys. Rev. Lett. **99**, 160502 (2007).

[76] S. F. Huelga, A. Rivas, and M. B. Plenio, Non-Markovianity-Assisted Steady State Entanglement, Phys. Rev. Lett. **108**, 160402 (2012).

[77] A. González-Tudela, V. Paulisch, D. E. Chang, H. J. Kimble, and J. I. Cirac, Deterministic Generation of Arbitrary Photonic States Assisted by Dissipation, Phys. Rev. Lett. **115**, 163603 (2015).

[78] K. Toyoda, Y. Matsuno, A. Noguchi, S. Haze, and S. Urabe, Experimental Realization of a Quantum Phase Transition of Polaritonic Excitations, Phys. Rev. Lett. **111**, 160501 (2013).

[79] R. Ohira, S. Kume, K. Takayama, S. Muralidharan, H. Takahashi, and K. Toyoda, Blockade of phonon hopping in trapped ions in the presence of multiple local phonons, Phys. Rev. A **103**, 012612 (2021).

[80] S. Debnath, N. M. Linke, S.-T. Wang, C. Figgatt, K. A. Landsman, L.-M. Duan, and C. Monroe, Observation of Hopping and Blockade of Bosons in a Trapped Ion Spin Chain, Phys. Rev. Lett. **120**, 073001 (2018).

[81] See Supplemental Material at http://link.aps.org/supplemental/10.1103/PhysRevLett.129.140501 for details about experimental setup, measurement of phonon numbers after sideband cooling, calibration of parameters and derivation of JCH model Hamiltonian, which includes Ref. [82].

[82] A. C. Lee, J. Smith, P. Richerme, B. Neyenhuis, P. W. Hess, J. Zhang, and C. Monroe, Engineering large Stark shifts for control of individual clock state qubits, Phys. Rev. A **94**, 042308 (2016).

[83] D. Leibfried, R. Blatt, C. Monroe, and D. Wineland, Quantum dynamics of single trapped ions, Rev. Mod. Phys. **75**, 281 (2003).